CROATICA CHEMICA ACTA
CCACAA, ISSN-0011-1643, ISSN-1334-417X
Croat. Chem. Acta **82** (1) (2009) 79-86.
CCA-3298

Original Scientific Paper

Assembling Screws: Large Preference for the Homochiral Combination in the Proton-Bound Dimers of 1-Aza[6]helicene in the Gas Phase*

Jiří Míšek,[a] Miloš Tichý,[a] Irena G. Stará,[a] Ivo Starý,[a,] Jana Roithová,[a,b,**] and Detlef Schröder[a,**]**

[a]*Institute of Organic Chemistry and Biochemistry, Flemingovo nám. 2, 16610 Prague 6, Czech Republic*
[b]*Department of Organic Chemistry, Faculty of Sciences, Charles University in Prague, Hlavova 8, 12843 Prague 2, Czech Republic*

RECEIVED JUNE 13, 2008; REVISED SEPTEMBER 23, 2008; ACCEPTED SEPTEMBER 29, 2008

Abstract. By means of selective deuterium labeling combined with separation of enantiomers, chiral discrimination in the proton-bound dimers of 1-aza[6]helicene is probed by electrospray mass spectrometry. The analysis of the results reveals a pronounced preference for the formation of homochiral dimers (*P,P* and *M,M*) over the heterochiral variant (*P,M*).

Keywords: azahelicenes, chiral discrimination, density functional theory, proton-bound dimers

INTRODUCTION

Ever since the structure of DNA was resolved, helical molecules attract attention in structural chemistry. Within recent years, a systematic synthesis of helicenes, *i.e.* prototype helical hydrocarbon molecules with all-ortho-fused aromatic rings,[1,2] has been developed which not only allows the synthesis of the pure hydrocarbons, but also provides access to a number of heteroatom derivatives.[3,4] Recently, we have initiated mass spectrometric studies of aza[6]helicenes, as one particular class of helicene derivatives, which have a heteroatom incorporated into the backbone.[5] Though having only a single nitrogen atom, 1- and 2-aza[6]helicene turned out having proton affinities (PAs) of about 1000 kJ mol^{-1}, and therefore these bases may be referred to as superbases.[6–11] In addition to their basicity, however, a particularly interesting feature of aza[6]helicenes is their helical chirality and in our first report, we already have demonstrated some enantioselective effects in the association of protonated aza[6]helicene with secondary alkanols,[5] which are particularly suitable chiral substrates for such gas-phase studies of chiral discrimination.[12–14] Here, we report an experimental study of the chiral discrimination in the formation of proton-bound homodimers of 1-aza[6]helicene (**1**) (Scheme 1) with paying particular attention to the experimental strategy to unravel chiral effects in the gas phase.

1

Scheme 1.

EXPERIMENTAL AND THEORETICAL METHODS

Synthesis of [7,8-D_2]-1-Aza[6]helicene

The synthesis of the deuterated 1-aza[6]helicene is based on the general strategy developed by some of us for the metal-mediated cyclotrimerization of an appropriate triyne followed by oxidative aromatization.[3,4] The deuterium label was introduced by base-promoted H/D exchange of the acetylenic protons (Scheme 2). Originally, the stepwise procedure with the isolation of products failed as the aqueous workup after quenching a lithium salt of **2** by deuterium oxide resulted in scrambling the isotope labels. Therefore, we performed the

* Dedicated to Professor Zvonimir Maksić on the occasion of his 70th birthday.
** Author to whom correspondence should be addressed. (E-mail: ivo.stary@uochb.cas.cz, jana.roithova@natur.cuni.cz, detlef.schroeder@uochb.cas.cz)

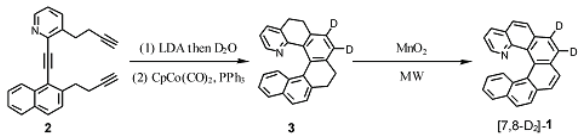

Scheme 2.

sequence **2** → **3** including the [2+2+2] cycloisomerization as a one-pot operation. Satisfactorily, the crude azahelicene derivative **3** could be oxidized with manganese dioxide in microwave oven to give the desired [7,8-D_2]-**1**. Although the deuteration at the 7- and 8-positions of the resulting azahelicene was incomplete (see below), it was fully sufficient for the mass spectrometric experiments described in the following.

For the synthesis of the deuterated 1-aza[6]helicene, a 20 ml glass vial was charged with diisopropylamine (20.2 mg, 200 μmol, 2.2 equiv.) in THF (5 ml) under argon and cooled to 0 °C. n-BuLi (1.6 M solution in hexanes, 124 μl, 200 μmol, 2.2 equiv.) was added dropwise and the mixture was stirred at 0 °C for 30 min. The solution was cooled to −78 °C, the triyne precursor **2** (30 mg, 90 μmol) in THF (5 ml) was added and the reaction mixture was stirred at −78 °C for 30 min. Then, D_2O (10 mg, 500 μmol, 5.6 equiv.) was added and the mixture was allowed to warm to room temperature. Subsequently, $CpCo(CO)_2$ (2.7 mg, 15 μmol, 0.17 equiv.) and PPh_3 (9.4 mg, 36 μmol, 0.40 equiv.) in THF (5 ml) were added and the reaction mixture was heated to 150 °C for 14 min. using microwave irradiation. Then, volatile components were removed *in vacuo* to yield crude **3**. Without further work-up the glass vial was charged with MnO_2 (235 mg, 2.70 mmol, 29.7 equiv.) and toluene (10 ml), tightly capped and heated by microwave irradiation to 150 °C for 80 min. The resulting reaction mixture was directly chromatographed on silica gel (hexane-acetone-triethylamine (80:20:1) to provide the azahelicene [7,8-D_2]-**1** (13 mg, 45 %) as an amorphous yellowish solid.

^{1}H NMR (500 MHz, $CDCl_3$) δ/ppm: 6.58 (1 H, ddd, J = 8.5, 6.8, 1.5 Hz), 7.10 (1 H, dd, J = 8.0, 4.2 Hz), 7.18 (1 H, ddd, J = 8.0, 6.8, 1.2 Hz), 7.56 (1 H, ddd, J = 8.6, 1.2, 0.6 Hz), 7.84 (1 H, ddd, J = 8.0, 1.5, 0.6 Hz), 7.85 (1 H, d, J = 8.5 Hz), 7.90 (1 H, s), 7.90 (1 H, s), 7.92 (1 H, dd, J = 4.2, 1.8 Hz), 7.98 (1 H, d, J = 8.2 Hz), 8.00 (1 H, d, J = 8.2 Hz), 8.02 (1 H, d, J = 8.5 Hz), 8.11 (1 H, dd, J = 8.0, 1.8 Hz); ^{13}C NMR (125 MHz, $CDCl_3$) δ/ppm: 120.56 (d), 124.13 (d), 124.20 (s), 124.66 (d), 125.99 (d), 126.01 (d), 126.23 (d), 126.29 (s), 126.35 (d), 127.15 (d), 127.48 (d), 127.83 (d), 128.11 (d), 128.69 (s), 129.80 (s), 130.96 (s), 131.15 (s), 131.85 (s), 133.01 (s), 133.21 (s), 135.07 (d), 145.84 (s), 146.73 (d); IR ($CHCl_3$): 3050 w, 2279 vw, 1613 w, 1598 w, 1574 w, 1553 w, 1515 w, 1496 w, 1397 w, 1366 w, 1304 w, 1262 w, 1134 m, 1115 m, 1096 m, 1076 m, 1040 m, 1027 m, 834 vs; EI MS *m/z*: 331 ($M^{+\cdot}$, 100), 330 (89), 329 (35), 304 (27), 303 (21), 302 (28), 256 (7), 164 (17), 151 (10), 111 (8), 97 (12), 83 (15), 69 (27), 57 (30), 43 (27). As detailed below, electrospray ionization mass spectra imply a deuterium incorporation of (80.5 ± 1.5) atom-% D in the 7- and 8-positions; HR EI-MS: calculated for $C_{25}H_{13}D_2N$: *m/z* = 331.1330; found: *m/z* = 331.1335.

^{1}H NMR spectra were measured at 500 MHz and ^{13}C NMR spectra at 125 MHz in $CDCl_3$ with TMS as an internal standard. Chemical shifts are given in δ-scale, coupling constants J are given in Hz. For correct assignment of the ^{1}H and ^{13}C NMR spectra, additional COSY, ROESY, HMQC, HMBC (with J_{C-H} = 5 Hz), and CIGAR-HMBC experiments were performed (not reported). IR spectra were measured in $CHCl_3$. EI MS spectra were recorded with 70 eV electrons, *m/z* values are given along with their relative intensities (%). HR MS spectra were obtained by EI. Commercially available reagent grade materials were used as received. Diisopropylamine was degassed by three freeze-pump-thaw cycles before use; toluene was distilled from calcium hydride under argon; THF was freshly distilled from sodium/benzophenone under nitrogen. TLC was performed on Silica gel 60 F_{254}-coated aluminium sheets (Merck) and spots were detected by the solution of $Ce(SO_4)_2 \cdot 4H_2O$ (1 %) and $H_3P(Mo_3O_{10})_4$ (2 %) in sulfuric acid (10 %). Flash chromatography was performed on Silica gel 60 (0.040−0.063 mm, Merck). The HPLC analysis of the chiral azahelicenes was performed on a Chiralcel OD-H column (250 × 4.6 mm, 5 μm) in heptane–isopropanol 3:1, flow rate 0.8 ml min^{-1}, with simultaneous UV detection at 254 nm (Varian) and polarimetric detection (Chiralizer, Knauer). The HPLC separation of the enantiomers of the azahelicenes was performed on a Eurocel 01 column (250 × 20 mm) in heptane–isopropanol 3:1, flow rate 19 ml min^{-1}, on-line UV detection at 254 nm (Agilent).

Optical Resolution of D_2-1-Aza[6]helicene

In HPLC on a Eurocel 01 column, both enantiomers of 1-aza[6]helicene differ enough in their retention times to be separated in a semipreparative way. Racemic azahelicene [7,8-D_2]-**1** (4 mg) was resolved by repeated HPLC separations using an Agilent 1100 Series preparative instrument (heptane-isopropanol 3:1, 19 ml min^{-1} flow rate, 0.5 mg injections of the racemate in 600 μl eluent). Evaporation of the solvents afforded (−)-(*M*)-[7,8-D_2]-**1** (1 mg, >99 % ee, retention time 9.2 min.) and (+)-(*P*)-[7,8-D_2]-**1** (1.5 mg, >99 % ee, retention time 10.7 min) as yellowish crystals. The absolute configuration of the labeled compounds was determined by comparison of their circular dichroism spectra with that of (+)-(*P*)-**1** whose absolute configuration has been determined by x-ray diffraction.

Electrospray Mass Spectrometry

The experiments were performed using the electrospray ionization source of a TSQ Classic mass spectrometer which has been described in detail elsewhere.[5,15] While only ion abundances in the source mass spectra are described below, the proton-bound dimers of the 1-aza[6]helicenes were also characterized by their collision-induced dissociation spectra, which show the exclusive decomposition to the protonated monomers. The proton-bound dimers were generated from mmolar solutions of the azahelicenes in pure methanol, which were introduced to the electrospray source *via* a syringe pump (*ca*. 5 μl min^{-1}). The ionization conditions were kept soft[16] in order to enhance the formation of proton-bound dimers.[17]

Computational Methods

The preliminary calculations employed the hybrid density functional method B3LYP[18–21] with the 6-31G** basis sets as implemented in Gaussian 03.[22] Geometries of four different structures for both homo- and heterochiral dimers were optimized and the harmonic frequencies were calculated in order to verify the minima and to obtain zero-point vibrational energies. The geometries were pre-optimized at the semiempirical level AM1. As stated below, a more relevant description of the stacking interactions in the proton-bound dimers would require more elaborate methods for the adequate description of dispersion interaction,[23] which are, however, prohibitive due to the size of the investigated system. In order to estimate the realistic relative energies, single-point calculations at the MP2/6-31G*(0.25)[24] level were performed for the optimized structures and the zero-point energies from the DFT calculations were used to obtain the final relative energies of the dimers.

RESULTS AND DISCUSSION

Electrospray ionization (ESI) of a methanolic solution of **1** gives rise to an intense signal corresponding to the protonated molecule $[\mathbf{1}+H]^+$, which can be attributed to the large basicity of the azahelicene. Upon adjustment of mild ionization conditions,[16,17] the ESI process can also lead to larger associates, namely, the proton-bound dimer $[\mathbf{1}_2+H]^+$ is generated in the present case. Upon collision-induced dissociation (CID) of mass-selected $[\mathbf{1}_2+H]^+$, cleavage of the hydrogen bond and thus loss of neutral helicene is observed exclusively. The apparent threshold of this process amounts to only about 0.3 eV.[25] In contrast, the threshold for dissociation of the covalent bonds in $[\mathbf{1}+H]^+$ is much larger (about 3 eV) and CID leads to a series of non-specific fragmentations (*e.g.* H_2, CH_3, and C_2H_4 losses).[26] Due to the inherent chirality of helicenes, the expectably relatively fragile proton-bound dimers of two helicenes with a heteroatom in the A-ring, for which $[\mathbf{1}_2+H]^+$ is an example, may thus represent a case in which a significant enantiomeric discrimination may be observed in the gas phase and possibly also in solution.

Prior to further addressing the results, some general comments on the experimental strategy are made. Specifically, mass spectrometry is an achiral method in that it cannot distinguish between enantiomeric molecules, because the effects of the various electromagnetic fields operative in a mass spectrometer are largely predominated by the real Coulomb charge of the ionic species.[27] Most strategies for the detection of chiral effects using mass spectrometry therefore require both: (i) the investigation of diastereomeric molecules (or clusters) and (ii) a conversion of the stereochemical information into mass differences.[28,29] Besides other approaches, selective isotopic labeling of one of the enantiomers represents a minimal perturbation of the system under investigation.[14] This effort requires a feasible synthetic route for introduction of an isotope label into the compounds of interest as well as the ability to prepare or separate the products in enantiomerically pure form; the latter condition inherently includes that the epimerization barrier is sufficiently high to avoid racemization upon handling at ambient conditions. With 1-aza[6]helicene, this task could be mastered by preparing a [7,8-D_2]-labeled compound followed by separation of the enantiomers on a chiral column (see experimental details). However, the sequence of the multistep synthesis of 1-aza[6]helicene with a base-promoted H/D exchange of a triyne prior to metal-mediated cyclotrimeri-

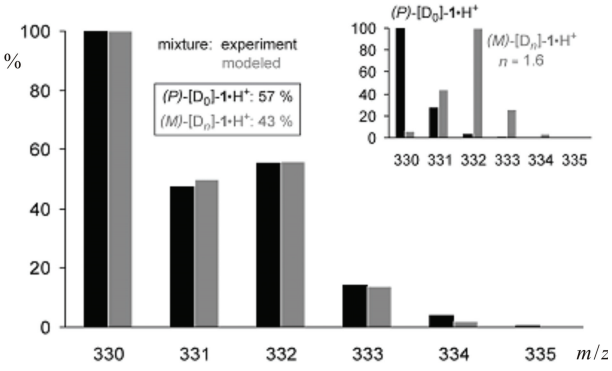

Figure 1. Normalized ion abundances of the mass region of the monomeric species of the protonated 1-aza[6]helicenes in the ESI mass spectrum of a *ca*. 1 : 1 mixture of *(P)*-[D_0]-**1** and *(M)*-[D_n]-**1**. The inset shows the isotope patterns of pure samples of *(P)*-[D_0]-**1** (black bars) and *(M)*-[D_n]-**1** (grey bars) measured separately; from the latter, the degree of deuteration is determined as $n = 1.61 \pm 0.03$ (see text). Fitting of the experimental spectrum of the prepared mixture (black bars) by a linear combination of the isotope patterns of the separate components (grey bars) reveals an actual mixing ratio of 57 : 43.

zation as the key step (Scheme 2) led to a somewhat lower incorporation of deuterium in the real sample, *i.e.* [D_n]-**1** compared to the desired target compound [7,8-D_2]-**1**. The incomplete deuteration thus adds a further complication to the interpretation of the experimental data.

Given the availability of both enantiomers in unlabeled as well as labeled form, the next step towards gas-phase experiments investigating possible chiral effects consists in the preparation of an artificial racemate by mixing one chiral sample in unlabeled form with its labeled enantiomer. However, from synthesis, enantiomer separation, and the required spectroscopic characterization, we had only a limited amount of sample available (*ca*. 0.4 mg) which is to be used for several series of experiments. Moreover, after recovery from the column and evaporation of the solvents used, in these quantities the 1-aza[6]helicene occurs as a thin, somewhat sticky layer on the surface of the flask, rather than forming to perfectly crystalline material. A gravimetric mixing scheme was therefore abandoned. Instead, the mixtures were prepared only roughly and the actual mixing ratio has been determined by means of ESI-MS. Figure 1 shows the experimental isotope patterns of one of the mixtures prepared as an example. Linear combination of the corresponding isotope envelopes of the separate components (see inset) allows the determination of the mixing ratio as (57 ± 1) : (43 ± 1): note that the isotope pattern of the pure compound *(M)*-[D_n]-**1** also allows the determination of the degree of deuteration of the sample, which is found to be n = 1.61 ± 0.03 or (80.5 ± 1.5) atom-% D.

Using this information as an input, the isotope cluster of the proton-bound dimer generated under mild ESI conditions can be analyzed quantitatively.[30] This kind of analysis is based on the following assumptions illustrated for the example of *(P)*-[D_0]-**1** and *(M)*-[D_n]-**1**, which are abbreviated as P and M, respectively, in the indexes of the following variables. (i) The proton-bound dimers are formed from the corresponding monomers proportional to their molar fractions x_P and x_M in the mixture (with $\Sigma x_i = 1$). (ii) In addition to the statistical preference, any kind of stereoselectivity in the formation of the dimers is acknowledged by inclusion of a stereochemical effect defined as $SE = K_{homo} / K_{hetero} = K_{PP} / K_{PM} = K_{MM} / K_{PM}$, where K_i stands for the respective equilibrium constants associated with formation of the proton-bound dimers. (iii) In order to account for equilibrium isotope effects (EIE), which have previously been found to be operative in gas-phase equilibrium measurements,[31] an EIE is allowed to act as a flexible parameter for each deuterium atom incorporated in the dimers. It is to be pointed out explicitly that his kind of analysis is derived from equilibrium kinetics, while electrospray ionization is a highly dynamic process and may thus lead to a non-equilibrium distribution of the ions evolving from the solution, *via* charged droplets to the gas phase.[32] In the present approach, however, the only difference between the constituents of the proton-bound dimers is their chirality. When comparing the results for the labeled and unlabeled ions for different mixtures of enantiomers, the non-equilibrium effects are likely to cancel out because the sole difference is the chirality of the compounds under study. In this context we further note that the equilibrium constants K_i as well as the equilibrium isotope effect (EIE) are to be regarded as the ratios of the respective sums of individual rates under non-equilibrium conditions rather than representing true equilibrium values. Once more, however, these differences can be assumed to cancel in the comparison of *(P)*- and *(M)*-enantiomers.

Within this framework, the intensities ($I_{m/z}$) of the dimers in the mass range from m/z = 659 to m/z = 666 can be modeled using the Eqs. (1)−(8), in which the terms $y_{P,m/z}$ and $y_{M,m/z}$ represent the molar fractions of the individual isotopes as derived from the measured isotope patterns of the monomeric species (see inset in Figure 1). Note that with respect to the experimental accuracy as well as vanishing intensities in the modeling, the EIE on the ^{13}C terms of *(M)*-[D_1]-**1**, the homochiral *(P,P)*-dimers with m/z > 662, the heterochiral *(P,M)*-dimers with m/z > 664, and the homochiral *(M,M)*-dimers with m/z > 666, were neglected for the sake of simplicity.

$$I_{659} = \left(x_M \bullet y_{M,330}\right)^2 + 2 \bullet x_M \bullet y_{M,330} \bullet x_P \bullet y_{P,330} + \left(x_P \bullet y_{P,330}\right)^2 \quad (1)$$

$$I_{660} = 2 \bullet x_M^2 \bullet y_{M,330} \bullet EIE \bullet y_{M,331} + 2 \bullet x_M \bullet y_{M,330} \bullet x_P \bullet y_{P,331} + 2 \bullet x_M \bullet EIE \bullet y_{M,331} \bullet x_P \bullet y_{P,330} + 2 \bullet x_P^2 \bullet y_{P,330} \bullet y_{P,331} \quad (2)$$

$$I_{661} = 2 \bullet x_M^2 \bullet y_{M,330} \bullet EIE^2 \bullet y_{M,332} + x_M^2 \bullet EIE^2 \bullet y_{M,331}^2 + 2 \bullet x_M \bullet y_{M,330} \bullet x_P \bullet y_{P,332} + 2 \bullet x_M \bullet EIE \bullet y_{M,331} \bullet x_P \bullet y_{P,331} + 2 \bullet x_M \bullet EIE^2 \bullet y_{M,332} \bullet x_P \bullet y_{P,330} + 2 \bullet x_P^2 \bullet y_{P,330} \bullet y_{P,332} + x_P^2 \bullet y_{P,331}^2 \quad (3)$$

$$I_{662} = 2 \bullet x_M^2 \bullet EIE^2 \bullet y_{M,330} \bullet y_{M,333} + 2 \bullet x_M^2 \bullet EIE^3 \bullet y_{M,331} \bullet y_{M,332} + 2 \bullet x_M \bullet y_{M,330} \bullet x_P \bullet y_{P,333} + 2 \bullet x_M \bullet EIE \bullet y_{M,331} \bullet x_P \bullet y_{P,332} + 2 \bullet x_M \bullet EIE^2 \bullet y_{M,332} \bullet x_P \bullet y_{P,331} + 2 \bullet x_M \bullet EIE^2 \bullet y_{M,333} \bullet x_P \bullet y_{P,330} + 2 \bullet x_P^2 \bullet y_{P,330} \bullet y_{P,333} + 2 \bullet x_P^2 \bullet y_{P,331} \bullet y_{P,332} \quad (4)$$

$$I_{663} = 2 \bullet x_M^2 \bullet EIE^2 \bullet y_{M,330} \bullet y_{M,334} + 2 \bullet x_M^2 \bullet EIE^3 \bullet y_{M,331} \bullet y_{M,333} + x_M^2 \bullet EIE^4 \bullet y_{M,332}^2 + 2 \bullet x_M \bullet EIE \bullet y_{M,331} \bullet x_P \bullet y_{P,333} + 2 \bullet x_M \bullet EIE^2 \bullet y_{M,332} \bullet x_P \bullet y_{P,332} + 2 \bullet x_M \bullet EIE^2 \bullet y_{M,333} \bullet x_P \bullet y_{P,331} + x_M \bullet EIE^2 \bullet y_{M,334} \bullet x_P \bullet y_{P,330} \quad (5)$$

$$I_{664} = 2 \bullet x_M^2 \bullet EIE^2 \bullet y_{M,330} \bullet y_{M,335} + 2 \bullet x_M^2 \bullet EIE^3 \bullet y_{M,331} \bullet y_{M,334} + 2 \bullet x_M^2 \bullet EIE^4 \bullet y_{M,332} \bullet y_{M,333} + 2 \bullet x_M \bullet EIE^2 \bullet y_{M,332} \bullet x_P \bullet y_{P,333} + 2 \bullet x_M \bullet EIE^2 \bullet y_{M,333} \bullet x_P \bullet y_{P,332} + 2 \bullet x_M \bullet EIE^2 \bullet y_{M,334} \bullet x_P \bullet y_{P,331} + 2 \bullet x_M \bullet EIE^2 \bullet y_{M,335} \bullet x_P \bullet y_{P,330} \quad (6)$$

$$I_{665} = 2 \bullet x_M^2 \bullet EIE^3 \bullet y_{M,331} \bullet y_{M,335} + 2 \bullet x_M^2 \bullet EIE^4 \bullet y_{M,332} \bullet y_{M,334} + x_M^2 \bullet EIE^4 \bullet y_{M,333}^2 \quad (7)$$

$$I_{666} = 2 \bullet x_M^2 \bullet EIE^4 \bullet y_{M,332} \bullet y_{M,335} + 2 \bullet x_M^2 \bullet EIE^4 \bullet y_{M,333} \bullet y_{M,334} \quad (8)$$

For the above example of the combination of the compounds *(P)*-[D_0]-**1** and *(M)*-[D_n]-**1**, the experimentally obtained isotope pattern as well as the modeled ion abundances are shown in Figure 2. A good fit of the experimental data can only be obtained, if a SE larger than 10 is assumed; for comparison, the inset shows the corresponding modeling for SE = 1. Further, the heavier dimers are slightly less abundant in the experiment than expected which can be acknowledged by assuming a phenomenological EIE of 0.93 per D atom.

In contrast, a control experiment with a mixture of *(M)*-[D_0]-**1** and *(M)*-[D_n]-**1** gives a good fit for SE = 1

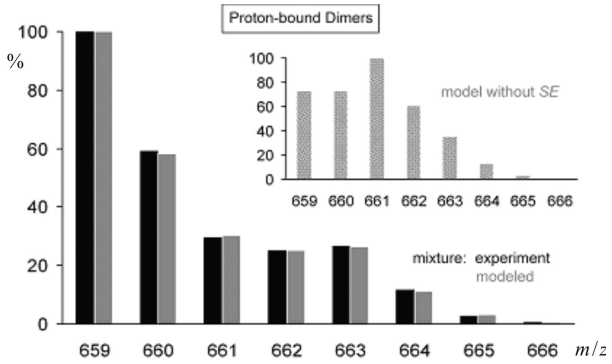

Figure 2. Normalized ion abundances of the mass region of the proton-bound dimers of the 1-aza[6]helicenes in the ESI mass spectrum of a 57 : 43 mixture of *(P)*-[D_0]-**1** and *(M)*-[D_n]-**1**. Fitting of the experimental data (black bars) by a linear combination of the mixing ratio with a stereochemical effect (grey bars) of provides a value of SE = 15 in favor of the homochiral complexes [*(P)*-[D_0]-**1**]$_2H^+$ over the statistically preferred heterochiral variant [*(P)*-[D_0]-**1**][*(M)*-[D_n]-**1**]H^+; in addition, a EIE of 0.93 per D atom is implied by the fitting. For comparison, the inset shows the modeled isotope patterns for the same mixture with SE = 1.

and EIE = 0.97 (Figure 3). Repeated measurements lead to averaged values of SE = 13 ± 2 and EIE = 0.95 ± 0.05. The small, normal isotope effect derived from the fitting of is not exceptional; note that the EIE might in part also reflect a slight discrimination of the heavier ions at the mass resolution required to properly separate the isotope cluster of the proton-bound dimers with a quadrupole mass analyzer.[33,34] The value of the SE is clearly significant, however, and among the largest enantiodiscriminations found so far with mass spectro-

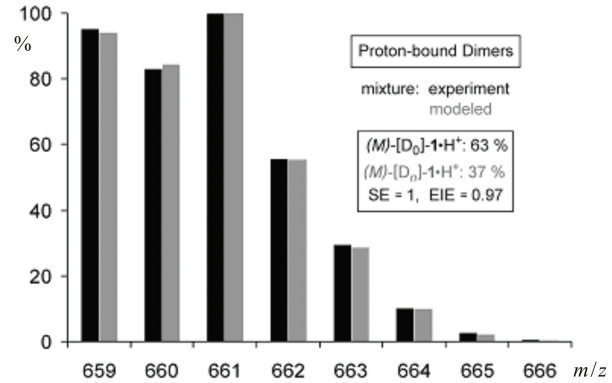

Figure 3. Normalized ion abundances of the mass region of the proton-bound dimers of a 63 : 37 mixture of *(M)*-[D_0]-**1** and *(M)*-[D_n]-**1**. Fitting of the experimental data (black bars) by a linear combination of the mixing ratio with a stereochemical effect set to a value of SE = 1 (grey bars) reproduces the experimental data reasonably well as expected for this control experiment; in addition, a EIE of 0.97 per D atom is applied.

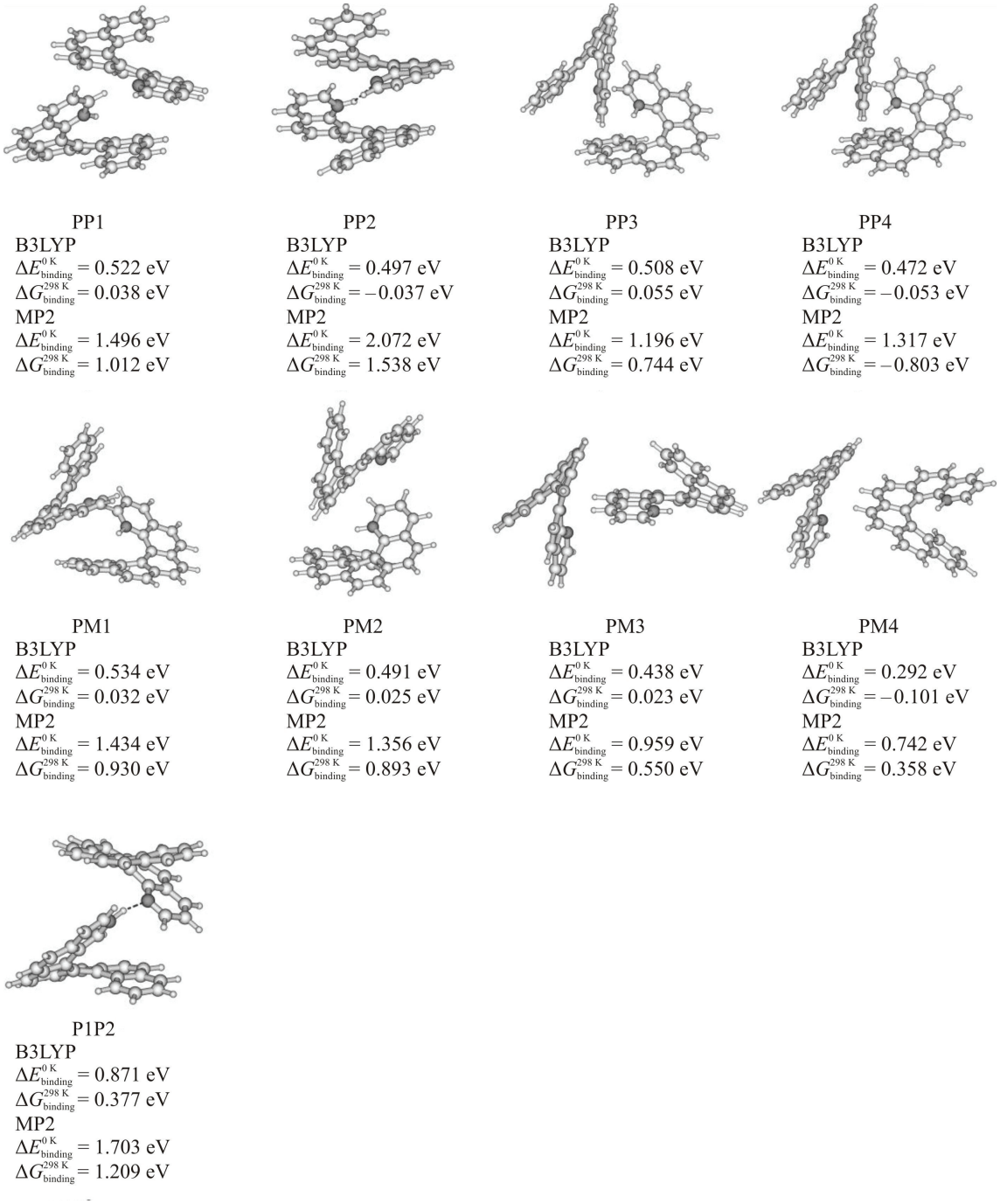

Figure 4. Structures of the homo- (*P,P*)- and heterochiral (*P,M*)- proton-bound dimers of the 1-aza[6]helicenes and (*P,P*)- proton-bound dimer of the 1-aza[6]helicene and 2-aza[6]helicene derived from B3LYP and MP2//B3LYP calculations. The binding energies refer to separated protonated helicene and a neutral helicene molecule. For the dimer P1P2, the value refers to protonated 1-aza[6]helicene and neutral 2-aza[6]helicene.

metric means for molecules with a single chiral center.[27–29,35–37]

In order to get a first idea about the origin of the large SE, the proton-bound dimer $[\mathbf{1}_2+H]^+$ was investigated using the semi-empirical AM1 method followed by optimization of the geometries of the dimers using density functional hybrid method B3LYP. Figure 4 shows four isomers of homochiral (PP1–PP4) and heterochiral dimers (PM1–PM4). All structures reveal an important aspect of helicenes, which is the highly delocalized electronic structure. Thus, the positive charge created upon protonation of one molecule of helicene is

delocalized, *via* polarization, over the entire skeleton and the interaction with the second helicene is therefore only little specific at least at the B3LYP level, which may not correctly describe the dispersion interaction between the aromatic backbones of the helicene molecules. The nitrogen atoms are moreover "hidden" inside the helical backbones and therefore the direct binding of the nitrogen atoms of two 1-aza[6]helicene molecules *via* the proton is sterically hindered. The effect of the steric hindrance can be illustrated on the dimer P1P2, in which **1** is bound to the isomeric 2-aza[6]helicene. The binding energy is almost doubled.

The effect of the dispersion interaction is estimated by single-point calculations at the MP2/6-31G*(0.25) level, where the basis set is altered so that the d orbitals on the carbon and nitrogen atoms are more delocalized in order to better describe the long-range interactions. At the first sight, the dispersion interaction in this system plays a dominant role.[38,39] While the B3LYP Gibbs free energies of binding at 298 K are almost thermoneutral, the values obtained from the MP2 calculations suggest relatively large binding energies. Due to the dominant role of the dispersion interaction, the isomer PP2 with the best arrangement of the aromatic backbones and the N−H−N bridge represents the most stable homochiral dimer. The arrangement of the aromatic rings in the backbones resembles the arrangement in a benzene dimer with a parallel displaced geometry.[40] Similar arrangements can be found also in the isomers PP1, PM1, and PM2. Isomers PP3, PP4, PM3, and PM4 are apparently more loosely bound and the mutual interaction can be again compared to a simple model of a benzene dimer with T-shaped geometry, accordingly, these dimers lie considerably higher in energy. Note also that at the MP2 level, the binding energy between 1- and 2-aza[6]helicenes (isomer P1P2) drops below that of PP2, which is one more evidence for the dominant role of the dispersion interaction in the binding of the dimers.

Quite obviously, the PP2 dimer represents by far the most favored arrangement and explains the large experimental preference for the formation of the homochiral dimers. In comparison, even further optimization of the geometries of PM1 and PM2 at the MP2 level cannot result in a similarly favored stacked arrangements of the helical backbones due the their opposite orientations. Thus, although a full optimization of the geometries of the dimers at the appropriate level as well as an inclusion of the basis set superposition error calculations is necessary to obtain the correct binding energies, we believe that the present results already provide sufficient rationale for the observed experimental effects and further calculations will not change the general trend. The observed enantioselectivity in the formation of the proton-bound dimers of 1-aza[6]helicene is promising for further investigations in this direction.[35]

Acknowledgements. This work was supported by the Center for Biomolecules and Complex Molecular Systems (LC512), the Czech Academy of Sciences (Z40550506), the European Commission (FP6-015847), the Grant Agency of the Czech Republic (203/07/1664 and 203/08/1487), and the Ministry of Education of the Czech Republic (MSM0021620857).

REFERENCES

1. T. J. Katz, *Angew. Chem. Int. Ed.* **39** (2000) 1921–1923.
2. A. Urbano, *Angew. Chem. Int. Ed.* **42** (2003) 3986−3989.
3. F. Teplý, I. G. Stará, I. Starý, A. Kollárovič, D. Šaman, L. Rulíšek, and P. Fiedler, *J. Am. Chem. Soc.* **124** (2002) 9175−9180.
4. J. Míšek, F. Teplý, I. G. Stará, M. Tichý, D. Šaman, Císařová, P. Vojtíšek, and I. Starý, *Angew. Chem. Int. Ed.* **47** (2008) 3188−3191.
5. J. Roithová, D. Schröder, J. Míšek, I. G. Stará, and I. Starý, *J. Mass Spectrom.* **42** (2007) 1233−1237.
6. R. W. Alder, *J. Am. Chem. Soc.* **127** (2005) 7924−7931.
7. V. Raab, K. Harms, J. Sundermeyer, B. Kovačević, and Z. B. Maksić, *J. Org. Chem.* **68** (2003) 8790−8797.
8. V. Raab, E. Gauchenova, A. Merkoulov, K. Harms, J. Sundermeyer, B. Kovačević, and Z. B. Maksić, *J. Am. Chem. Soc.* **127** (2005) 15738−15743.
9. B. Kovačević and Z. B. Maksić, *Chem. Commun.* (2006) 1524−1526.
10. I. Kaljurand, I. A. Koppel, A. Kütt, E.-I. Rõõm, T. Rodima, I. Koppel, M. Mishima, and I. Leito, *J. Phys. Chem. A.* **111** (2007) 1245−1250.
11. Z. Glasovac, V. Štrukil, M. Eckert-Maksić, D. Schröder, M. Kacorowska, and H. Schwarz, *Int. J. Mass Spectrom.* **270** (2008) 39−46.
12. D. Schröder and H. Schwarz, *Int. J. Mass Spectrom*. **231** (2004) 139−146.
13. F. R. Novara, H. Schwarz, and D. Schröder, *Helv. Chim. Acta* **90** (2007) 2274−2280.
14. F. R. Novara, P. Gruene, D. Schröder, and H. Schwarz, *Chem. Eur. J.* **14** (2008) 5957.
15. J. Roithová and D. Schröder, *Phys. Chem. Chem. Phys.* **9** (2007) 731−738.
16. N. B. Cech and C. G. Enke, *Mass Spectrom. Rev.* **20** (2001) 362−387.
17. D. Schröder, M. Semialjac, and H. Schwarz, *Int. J. Mass Spectrom*. **233** (2004) 103−109.
18. A. D. Becke, *J. Chem. Phys*. **98** (1993) 5648−5652.
19. S. H. Vosko, L. Wilk, and M. Nusair, *Can. J. Phys.* **58** (1980) 1200−1211.
20. C. Lee, W. Yang, and R. G. Parr, *Phys. Rev. B* **37** (1988) 785−789.
21. B. Miehlich, A. Savin, H. Stoll, and H. Preuss, *Chem. Phys. Lett.* **157** (1989) 200−206.
22. M. J. Frisch, G. W. Trucks, H. B. Schlegel, G. E. Scuseria, M. A. Robb, J. R. Cheeseman, V. G. Zakrzewski, J. J. A. Montgomery, T. Vreven, K .N. Kudin, J. C. Burant, J. M. Millam, S. S. Iyengar, J. Tomasi, V. Barone, B. Mennucci, M. Cossi, G. Scalmani, N. Rega, G. A. Petersson, H. Nakatsuji, M. Hada, M. Ehara, K. Toyota, R. Fukuda, J. Hasegawa, M. Ishida, T. Nakajima, Y. Honda, O. Kitao, C. Adamo, J. Jaramillo, R. Gomperts, R. E. Stratmann, O. Yazyev, J. Austin, R. Cammi, C. Pomelli, J. Ochterski, P. Y. Ayala, K. Morokuma, G. A. Voth, P. Salvador,

J. J. Dannenberg, V. G. Zakrzewski, S. Dapprich, A. D. Daniels, M. C. Strain, O. Farkas, D. K. Malick, A. D. Rabuck, K. Raghavachari, J. B. Foresman, J. V. Ortiz, Q. Cui, A. G. Baboul, S. Clifford, J. Cioslowski, B. B. Stefanov, G. Liu, A. Liashenko, P. Piskorz, I. Komaromi, R .L. Martin, D. J. Fox, T. Keith, M. A. Al-Laham, C. Y. Peng, A. Nanayakkara, M. Challacombe, P. M. W. Gill, B. Johnson, W. Chen, M. W. Wong, C. Gonzalez, and J. A. Pople, *Gaussian03*, Revision C.02 ed.; Gaussian, Inc.: Wallingford CT, 2004.

23. J. Šponer and P. Hobza, *Coll. Czech. Chem. Commun.* **68** (2003) 2231−2282.
24. L. M. J. Kroon-Batenburg and F. B. van Duijneveldt, *J. Mol. Struct.* **121** (1985) 185.
25. B. Jagoda-Cwiklik, P. Jungwirth, L. Rulíšek, P. Milko, J. Roithová, J. Lemaire, P. Maitre, J. M. Ortega, and D. Schröder, *ChemPhysChem* **8** (2007) 1629−1639.
26. See also: M. Rentzea, M. Diehm, and H. A. Staab, *Tetrahedron Lett*. **35** (1994) 8361−8364.
27. J. S. Splitter and F. Tureček (Eds.), *Applications of Mass Spectrometry to Organic Stereochemistry*, VCH, Weinheim, 1994.
28. D. Schröder and H. Schwarz, *Top. Curr. Chem.* **225** (2003) 133−152.
29. M. Speranza, *Int. J. Mass Spectrom.* **232** (2004) 277−317.
30. D. Schröder, H. Schwarz, S. Schenk, and E. Anders, *Angew. Chem. Int. Ed.* **42** (2003) 5087−5090.
31. D. Schröder, R. Wesendrup, R. H. Hertwig, T. Dargel, H. Grauel, W. Koch, B. R. Bender, and H. Schwarz, *Organometallics* **19** (2000) 2608−2615.
32. N. G. Tsierkezos, J. Roithová, D. Schröder, M. Ončák, and P. Slavíček, *Inorg. Chem.* **48** (2009), in press (DOI:10.1021/ic900575r).
33. J. Roithová, P. Milko, C. L. Ricketts, D. Schröder, T. Besson, V. Dekoj, and M. Bělohradský, *J. Am. Chem. Soc.* **129** (2007) 10141−10148.
34. B. Colasson, M. Save, O. Reinaud, P. Milko, J. Roithová, and D. Schröder, *Org. Lett.* **9** (2007) 4987−4990.
35. J. Roithová, *Coll. Czech Chem. Commun.* **74** (2009) 243.
36. J. Míšek, M. Tichý, I. G. Stará, I. Starý, and D. Schröder, *Coll. Czech Chem. Commun.* **74** (2009) 323.
37. See also: S. C. Nanita and R. G. Cooks, *Angew. Chem. Int. Ed.* **45** (2006) 554−569.
38. S. Grimme, *Angew. Chem. Int. Ed.* **47** (2008) 3430−3434.
39. T. Smith, J. E. Del Bene, and L. Radom, *J. Am. Chem. Soc.* **112** (2007) 5286−5294.
40. E. C. Lee, D. Kim, P. Jurecka, P. Tarakeshwar, P. Hobza, and K. S. Kim, *J. Phys. Chem. A* **111** (2007) 3446−3457.

SAŽETAK

Stvaranje vijaka: velika preferencija za homokiralnu kombinaciju u protonom povezanim dimerima 1-aza[6]helicena u plinskoj fazi

Jiří Míšek,[a] Miloš Tichý,[a] Irena G. Stará,[a] Ivo Starý,[a] Jana Roithová[a,b] i Detlef Schröder[a]

[a]*Institute of Organic Chemistry and Biochemistry, Flemingovo nám. 2, 16610 Prague 6, Czech Republic*

[b]*Department of Organic Chemistry, Faculty of Sciences, Charles University in Prague, Hlavova 8, 12843 Prague 2, Czech Republic*

Pomoću selektivnog obilježavanja deuterijem, kombiniranim s razdvajanjem enantiomera, ispitivana je kiralna diskriminacija u protonom povezanim dimerima 1-aza[6]helicena s metodom elektrosprej masene spektrometrije. Analiza rezultata pokazuje naglašenu preferenciju za stvaranje homokiralnih dimera (*P*,*P* i *M*,*M*) u odnosu na heterokiralnu varijantu (*P*,*M*).